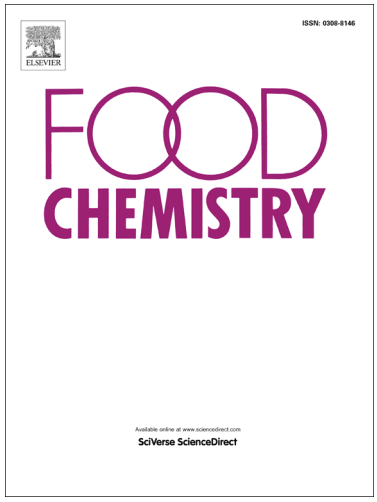

Novel hydroxypyridinone derivatives containing an oxime ether moiety: synthesis, inhibition on mushroom tyrosinase and application in anti-browning of fresh-cut apples

Le-Le Shao, Xiao-Ling Wang, Kai Chen, Xiao-Wu Dong, Li-Min Kong, De-Yin Zhao, Robert C Hider, Tao Zhou

PII: S0308-8146(17)31509-1
DOI: http://dx.doi.org/10.1016/j.foodchem.2017.09.054
Reference: FOCH 21723

To appear in: *Food Chemistry*

Received Date: 31 March 2017
Revised Date: 5 September 2017
Accepted Date: 11 September 2017

Please cite this article as: Shao, L-L., Wang, X-L., Chen, K., Dong, X-W., Kong, L-M., Zhao, D-Y., Hider, R.C., Zhou, T., Novel hydroxypyridinone derivatives containing an oxime ether moiety: synthesis, inhibition on mushroom tyrosinase and application in anti-browning of fresh-cut apples, *Food Chemistry* (2017), doi: http://dx.doi.org/10.1016/j.foodchem.2017.09.054

Novel hydroxypyridinone derivatives containing an oxime ether moiety: synthesis, inhibition on mushroom tyrosinase and application in anti-browning of fresh-cut apples

Le-Le Shao[a], Xiao-Ling Wang[b], Kai Chen[a], Xiao-Wu Dong[c], Li-Min Kong[a], De-Yin Zhao[a], Robert C Hider[d], Tao Zhou[a,*]

[a.] *School of Food Science and Biotechnology, Zhejiang Gongshang University, 18 Xuezheng Street, Xiasha, Hangzhou, Zhejiang 310018, P. R. China.*

[b.] *Faulty of Food Science, Zhejiang Pharmaceutical College, 888 East of Yinxian Road, Ningbo, Zhejiang,315100, P. R. China.*

[c.] *Zhejiang Province Key Laboratory of Anti-Cancer Drug Research, College of Pharmaceutical Sciences, Zhejiang University, Hangzhou 310058, P. R. China*

[d.] *Institute of Pharmaceutical Sciences, King's College London, 150 Stamford Street, London, SE1 9NH, UK*

* Corresponding author. Tel: (+86) 571 28008976; fax: (+86) 571 88905733. E-mail address: taozhou@zjgsu.edu.cn (T. Zhou).

Running title: Inhibition on tyrosinase and anti-browning of fresh-cut apples

Abstract: A range of hydroxypyridinone derivatives were synthesized starting from kojic acid. Among them, **10** and **11** were found to possess the strongest inhibitory effect on monophenolase activity of mushroom tyrosinase, having IC_{50} values of 2.04 and 1.60 μM, respectively. The IC_{50} values of **10** and **11** for the inhibition of diphenolase activity of mushroom tyrosinase were determined as 13.89 and 7.99 μM, respectively. Investigation of the inhibitory mechanism of these two compounds indicated that the inhibition was reversible and of a competitive-uncompetitive mixed type. The K_I and K_{IS} values of **10** were determined to be 24.84 and 32.54 μM, respectively, and the corresponding values for **11** being 18.07 and 21.34 μM, respectively. The effect of **11** on the browning process of fresh-cut apples was evaluated by measuring the color change and browning index. The results indicated that **11** had a significant effect on controlling the browning of fresh-cut apple slices.

Keywords: Hydroxypyridinone; Oxime ether; Tyrosinase; Inhibitor; Anti-browning

1. Introduction

With increased fast-pace lifestyles of modern time, fresh-cut apples are popular due to the advantages of freshness, convenience and nutrition (Allende, Tomás-Barberán, & Gil, 2006; Chen, Xing, Wang, Zheng, & Wang, 2015). However, the shelf-life of fresh-cut products is greatly shortened as compared with intact fruits and vegetables, because fresh-cut leads to tissue wounding (Chung & Moon, 2009). Among the negative consequences of wounding in fresh-cut products, enzymatic browning is considered to be one of the main limitations on the shelf-life of fresh-cut products (Brecht, 1995). It is estimated that over 50% loss of fruit and vegetables is due to enzymatic browning (Mosneaguta, Alvarez, & Barringer, 2012). Enzymatic browning of fresh-cut produce which appears along the cutting side is known to be mainly caused by polyphenol oxidase (PPO) and peroxidase (POD) catalyzed oxidation (Tomás-Barberán & Espín, 2001).

Tyrosinase (EC 1.14.18.1), also known as PPO, is a copper-containing monooxygenase that is widely distributed in microorganisms, animals, and plants (Hamidian, et al., 2013). Six histidine residues, located on a four helical bundle, coordinate two copper ions, which serve as the major cofactors in the active site (Zhao, et al., 2016). As a key enzyme of melanogenesis, tyrosinase catalyzes the hydroxylation of $_{L}$-tyrosinase ($_{L}$-Tyr) to $_{L}$-dihydroxyphenylalanine ($_{L}$-DOPA) (monophenolase activity) and further the oxidation of $_{L}$-DOPA to DOPA quinone (diphenolase activity). It is responsible for the undesirable enzymatic browning of fruits and vegetables that takes place during senescence or damage at the time of post-harvest handling (Liu, Shu, Liu, Huang, & Peng,

2016). On the one hand, the phenolic compounds in the food stuff are oxidized by PPO to form brown pigments, which can cause the browning of fruits and vegetables (Mayer, 2006). On the other hand, the oxidation products of phenolic compounds can react with other food components, including amines, peptides and proteins (Chen, Xing, Wang, Zheng, & Wang, 2015), which further reduces the food quality. Up to now, numerous tyrosinase inhibitors identified from both natural and synthetic origins have been reported (Chang, 2009; Kim & Uyama, 2005), but only a few are sufficiently potent for practical use due to poor inhibitory activity, solubility, instability, and safety concerns (Zheng, Zhang, Zhang, & Chen, 2015). Therefore, searching for novel and safe powerful tyrosinase inhibitors remains a challenge to the food and pharmaceutical industries.

Kojic acid (**1**), 5-hydroxy-2-(hydroxymethyl)-4H-pyran-4-one, a metabolic product of many species of *Aspergillus* and *Penicillium* moulds., has been used as an anti-browning agent in foods that rapidly change color (Li, et al., 2013). It was reported that application of kojic acid in the pre-storage of litchi fruit can delay pericarp browning and maintain the activities of antioxidative enzymes (Shah, Khan, & Ali, 2017). Application of kojic acid in combination with 4-hexylresocrinol and $_{L}$-cysteine effectively reduced the browning in “Amasya” apple juice (İyidoğan & Bayındırlı, 2004). As kojic acid can inhibit tyrosinase by chelating the copper ion in the active site of tyrosinase, modification of kojic acid provides a potential route for superior tyrosinase inhibitors (Lee, Park, Kim, Seo, & Kim, 2006; Noh, et al., 2009; Kwak, Choi, Park, & Lee, 2011). Hydroxypyridinones, are closely related to kojic acid, and have several

potential applications in the medicine area. Hydroxypyridinones bind copper with superior affinity to that of kojic acid, thus they can in principle inhibit tyrosinase activity by binding copper ions coordinated in the active site of the enzyme. Indeed, in our previous work some hydroxypyridinones were demonstrated to possess stronger anti-tyrosinase activity than kojic acid (Li, et al., 2013; Zhao, et al., 2016). Hydroxypyridinone derivatives have also been demonstrated to have potential applications in the preservation of shrimp and surimi product (Xu, et al., 2014; Dai, et al., 2016; Chen, et al., 2016). In order to search for stronger tyrosinase inhibitors, in this study, a series of novel hydroxypyridinone derivatives containing an oxime ether moiety were synthesized. The inhibitory effects on mushroom tyrosinase and on the browning process of fresh-cut apples of hydroxypyridinone derivatives containing an oxime ether moiety were also investigated.

2. Materials and Methods

2.1. Reagents

Tyrosinase from mushroom (lyophilized powder, ⩾1000 unit/mg solid) was purchased from Sigma. Kojic acid, L-tyrosinase (L-Tyr) and L-3,4-dihydroxyphenylalanine (L-DOPA) were the products of Aladdin (Shanghai, China). All other reagents were of analytical grade.

2.2. General Synthesis

The products were identified by NMR, ESI-MS and HRMS. ^{1}H NMR and ^{13}C NMR spectra were recorded on a Bruker Avance 500 spectrometer (Bruker Corp., Germany) with tetramethylsilane as an internal standard. Electrospray ionization (ESI) mass spectra were obtained by infusing samples into an LCQ Deca XP ion-trap instrument (ThermoFinnigan, San Jose, CA). High-resolution mass spectra (HRMS) were obtained on a QTOFMicro (Waters, U.S.) by direct infusing samples into the ESI source.

*Synthesis of 5-(Benzyloxy)-2-(hydroxymethyl)pyridin-4(1H)-one (**3a**).* Compound **2** (10.0 g) was dissolved in ethanol (17 mL) and the mixture was heated to reflux, then ammonia solution (25-28%, 83 mL) was added. The reaction mixture was refluxed overnight until the reaction was complete. After the reaction mixture was cooled to the room temperature, the precipitate was collected by filtration, washed twice with a small amount of diethyl ether and dried, providing the product compound **3a** as a white solid.

Compounds **2** and **3b-3f** were prepared according to our reported method (Li, et al., 2013).

*General Procedure for the Synthesis of **4**.* Compound **3** (4 mmol) was dissolved in CH_2Cl_2 (20 mL) and activated manganese (IV) oxide (32 mmol) was added. The reaction mixture was stirred vigorously for 3 days at room 50 ^{o}C and monitored by TLC. After completion of the reaction, the mixture was filtered to remove the activated manganese (IV) oxide powder, and the filtrate was dried under vacuum to give the product **4**.

*5-(benzyloxy)-4-oxo-1,4-dihydropyridine-2-carbaldehyde (**4a**):* Yield 61%. ^{1}H NMR (500 MHz, DMSO-d_6) δ: 5.31 (s, 2H, CH_2), 7.34-7.49(m, 6H, Ph and C3-H in

pyridinone ring), 8.42 (s, 1H, C6-H in pyridinone ring), 9.25 (s, 1H, CHO). ESI-MS: *m/z* 230 (MH^+).

*5-(benzyloxy)-1-methyl-4-oxo-1,4-dihydropyridine-2-carbaldehyde (**4b**):* Yield 72%. ^{1}H NMR (500 MHz, DMSO-d_6) δ: 2.49 (s, 3H, CH_3), 5.28 (s, 2H, CH_2), 7.00 (s, 2H, C3-H and C6-H in pyridinone), 7.29-7.45 (m, 5H, Ph), 9.75 (s, 1H, CHO). ESI-MS: *m/z* 244 (MH^+).

*5-(benzyloxy)-1-ethyl-4-oxo-1,4-dihydropyridine-2-carbaldehyde (**4c**):* Yield 74%. ^{1}H NMR (500 MHz, DMSO-d_6) δ: 1.27 (t, J = 7.0 Hz, 3H, CH_3), 4.24 (q, J = 7.0 Hz, 2H, CH_2), 5.25 (s, 2H, CH_2), 7.00 (s, 2H, C3-H and C6-H in pyridinone), 7.29-7.40 (m, 5H, Ph), 9.59 (s, 1H, CHO). ESI-MS: *m/z* 258 (MH^+).

*5-(benzyloxy)-1-butyl-4-oxo-1,4-dihydropyridine-2-carbaldehyde (**4d**):* Yield 76%. ^{1}H NMR (500 MHz, DMSO-d_6) δ: 0.86 (t, J = 7.5 Hz, 3H, CH_3), 1.13-1.21 (m, 2H, CH_2), 1.51-1.57 (m, 2H, CH_2), 4.18 (t, J = 7.5 Hz, 2H, CH_2), 5.25 (s, 2H, CH_2), 6.96 (1H, C3-H in pyridinone), 6.97 (s, 1H, C6-H in pyridinone), 7.30-7.40 (m, 5H, Ph), 9.58 (s, 1H, CHO). ESI-MS: *m/z* 286 (MH^+).

*5-(benzyloxy)-1-hexyl-4-oxo-1,4-dihydropyridine-2-carbaldehyde (**4e**):* Yield 76%. ^{1}H NMR (500 MHz, DMSO-d_6) δ: 0.87 (t, J = 7.0 Hz, 3H, CH_3), 1.23 (m, 6H, CH_2),1.56 (m, 2H, CH_2), 4.17 (t, J = 7.0 Hz, 2H, CH_2), 5.26 (s, 2H, CH_2), 6.97(s, 1H, C3-H in pyridinone ring), 6.99 (s, 1H, C6-H in pyridinone ring), 7.30-7.41(m, 5H, Ph), 9.58 (s, 1H, CHO). ESI-MS: *m/z* 314 (MH^+).

*5-(benzyloxy)-1-octyl-4-oxo-1,4-dihydropyridine-2-carbaldehyde (**4f**):* Yield 78%. ^{1}H NMR (500 MHz, DMSO-d_6) δ: 0.88 (t, J = 7.0 Hz, 3H, CH_3), 1.17-1.28 (m, 10H, $5CH_2$), 1.56 (m, 2H, CH_2), 4.17 (t, J = 7.0 Hz, 2H, CH_2), 5.26 (s, 2H, CH_2), 6.97 (s, 1H, C3-H in pyridinone), 6.98 (s, 1H, C6-H in pyridinone), 7.30-7.41 (m, 5H, Ph), 9.58 (s, 1H, CHO). ESI-MS: *m/z* 342 (MH^+).

*General Procedure for the Synthesis of **5**.* Compound **4** (2 mmol) was dissolved in EtOH/H_2O (10 mL/10 mL) and ethoxyamine hydrochloride (3 mmol) was added. The reaction mixture was stirred until all the solid was dissolved under ice bath. The ice bath was removed after NaOH solution (0.22 g in 10 mL of H_2O) was added dropwise, and the reaction mixture was stirred for 2 h at room temperature. After completion of the reaction, the mixture was concentrated to about half volume, and extracted with CH_2Cl_2 (3 × 30 mL). The combined organic layers were concentrated, and the resulting residue was purified by silica gel column chromatography (CH_2Cl_2/CH_3OH, 15:1) to provide the product **5**.

*5-(benzyloxy)-4-oxo-1,4-dihydropyridine-2-carbaldehyde O-ethyl oxime (**5a**):* Yield 71%. ^{1}H NMR (500 MHz, DMSO-d_6) δ: 1.24 (t, J = 7.0 Hz, 3H, CH_3), 4.16 (q, J = 7.0 Hz, 2H, CH_2), 5.14 (s, 2H, CH_2), 7.31-7.46(m, 5H, Ph), 7.97 (s, 1H, CH). ESI-MS: m/z 273 (MH^+).

*5-(benzyloxy)-1-methyl-4-oxo-1,4-dihydropyridine-2-carbaldehyde O-ethyl oxime (**5b**):* Yield 64%. ^{1}H NMR (500 MHz, $CDCl_3$) δ: 1.31 (t, J = 7.0 Hz, 3H, CH_3), 3.68 (s, 3H, CH_3), 4.24 (q, J = 7.0 Hz, 2H, CH_2), 5.20 (s, 2H, CH_2), 6.66 (s, 1H, C3-H in

pyridinone ring), 6.93 (s, 1H, C6-H in pyridinone ring), 7.29-7.42 (m, 5H, Ph), 7.91 (s, 1H, CH). ESI-MS: *m/z* 287 (MH^+).

*5-(benzyloxy)-1-ethyl-4-oxo-1,4-dihydropyridine-2-carbaldehyde O-ethyl oxime (**5c**):* Yield 61%. ^{1}H NMR (500 MHz, $CDCl_3$) δ: 1.26 (t, *J* = 7.0 Hz, 3H, CH_3), 1.30 (t, *J* = 7.0 Hz, 3H, CH_3), 4.00 (q, *J* = 7.0 Hz, 2H, CH_2), 4.23 (q, *J* = 7.0 Hz, 2H, CH_2), 5.19 (s, 2H, CH_2), 6.65 (s, 1H, C3-H in pyridinone ring), 6.93 (s, 1H, C6-H in pyridinone ring), 7.27-7.41 (m, 5H, Ph), 7.90 (s, 1H, CH). ESI-MS: *m/z* 301 (MH^+).

*5-(benzyloxy)-1-butyl-4-oxo-1,4-dihydropyridine-2-carbaldehyde O-ethyl oxime (**5d**):* Yield 71%. ^{1}H NMR (500 MHz, $CDCl_3$) δ: 0.87 (t, *J* = 7.5 Hz, 3H, CH_3), 1.12-1.22 (m, 2H, CH_2), 1.31 (t, *J* = 7.0 Hz, 3H, CH_3), 1.50-1.61 (m, 2H, CH_2), 3.93 (t, *J* = 7.5 Hz, 2H, CH_2), 4.23 (q, *J* = 7.0 Hz, 2H, CH_2), 5.21 (s, 2H, CH_2), 6.68 (s, 1H, C3-H in pyridinone ring), 6.89 (s, 1H, C6-H in pyridinone ring), 7.27-7.41 (m, 5H, Ph), 7.90 (s, 1H, CH). ESI-MS: *m/z* 329 (MH^+).

*5-(benzyloxy)-1-hexyl-4-oxo-1,4-dihydropyridine-2-carbaldehyde O-ethyl oxime (**5e**):* Yield 63%. ^{1}H NMR (500 MHz, $CDCl_3$) δ: 0.87 (t, *J* = 7.5 Hz, 3H, CH_3), 1.10-1.27 (m, 6H, $3CH_2$), 1.31 (t, *J* = 7.0 Hz, 3H, CH_3), 1.51-1.62 (m, 2H, CH_2), 3.92 (t, *J* = 7.5 Hz, 2H, CH_2), 4.23 (q, *J* = 7.0 Hz, 2H, CH_2), 5.21 (s, 2H, CH_2), 6.66 (s, 1H, C3-H in pyridinone ring), 6.90 (s, 1H, C6-H in pyridinone ring), 7.27-7.41 (m, 5H, Ph), 7.90 (s, 1H, CH). ESI-MS: *m/z* 357 (MH^+).

*5-(benzyloxy)-1-octyl-4-oxo-1,4-dihydropyridine-2-carbaldehyde O-ethyl oxime (**5f**):* Yield 74%. ^{1}H NMR (500 MHz, $CDCl_3$) δ: 0.87 (t, *J* = 7.5 Hz, 3H, CH_3), 1.10-1.27 (m,

10H, 5CH_2), 1.30 (t, *J* = 7.0 Hz, 3H, CH_3), 1.52-1.61 (m, 2H, CH_2), 3.90 (t, *J* = 7.5 Hz, 2H, CH_2), 4.22 (q, *J* = 7.0 Hz, 2H, CH_2), 5.19 (s, 2H, CH_2), 6.65 (s, 1H, C3-H in pyridinone ring), 6.90 (s, 1H, C6-H in pyridinone ring), 7.25-7.40 (m, 5H, Ph), 7.88 (s, 1H, CH). ESI-MS: *m/z* 385 (MH^+).

General Procedure for the Synthesis of ***6-11***. To a solution of compound **5** (1 mmol) in methanol (2 mL) was added hydrochloric acid solution (3 mL, 3 M). The mixture was heated to reflux for 36-72 h. After completion of the reaction, the mixture was extracted with CH_2Cl_2 (3 × 10 mL) and the combined organic layer was dried under vacuum to give the desired products as white solids.

*5-hydroxy-4-oxo-1,4-dihydropyridine-2-carbaldehyde O-ethyl oxime (**6**):* Yield 85%, white solid. ^{1}H NMR (500 MHz, DMSO-d_6) δ: 1.28 (t, *J* = 7.0 Hz, 3H, CH_3), 4.27 (q, *J* = 7.0 Hz, 2H, CH_2), 7.53 (s, 1H, C3-H in pyridinone ring), 8.16 (s, 1H, C6-H in pyridinone ring), 8.37 (s, 1H, CH). ^{13}C NMR (125 MHz, DMSO-d_6) δ: 14.80, 71.22, 110.44, 127.79, 137.84, 141.77, 146.34, 161.25. ESI-MS: *m/z* 183 (MH^+), HRMS: *m/z* calcd for $C_8H_{11}N_2O_3$ (MH^+) 183.0770, found 183.0779.

*5-hydroxy-1-methyl-4-oxo-1,4-dihydropyridine-2-carbaldehyde O-ethyl oxime (**7**):* Yield 85%, white solid. ^{1}H NMR (500 MHz, DMSO-d_6) δ: 1.29 (t, *J* = 7.0 Hz, 3H, CH_3), 4.08 (s, 3H, CH_3), 4.28 (q, *J* = 7.0 Hz, 2H, CH_2), 7.64 (s, 1H, C3-H in pyridinone ring), 8.29 (s, 1H, C6-H in pyridinone ring), 7.91 (s, 1H, CH). ^{13}C NMR (125 MHz, DMSO-d_6, δppm) δ: 14.82, 44.55, 71.27, 110.72, 133.39, 139.68, 142.07, 146.34, 160.21. ESI-MS: *m/z* 197 (MH^+), HRMS: *m/z* calcd for $_9H_{13}N_2O_3$ (MH^+) 197.0926, found 197.0937.

*1-ethyl-5-hydroxy-4-oxo-1,4-dihydropyridine-2-carbaldehyde O-ethyl oxime (**8**):*

Yield 86%, white solid. ^{1}H NMR (500 MHz, DMSO-d_6) δ: 1.29 (t, J = 7.5 Hz, 3H, CH_3), 1.34 (t, J = 7.5 Hz, 3H, CH_3), 4.28 (q, J = 7.5 Hz, 2H, CH_2), 4.47 (q, J = 7.5 Hz, 2H, CH_2), 7.64 (s, 1H, C3-H in pyridinone ring), 8.35 (s, 1H, C6-H in pyridinone ring), 8.63 (s, 1H, CH). ^{13}C NMR (125 MHz, DMSO-d_6) δ: 14.82, 16.53, 51.96, 71.29, 111.50, 132.14, 138.84, 141.86, 146.71, 160.48. ESI-MS: *m/z* 211 (MH^+), HRMS: *m/z* calcd for $C_{10}H_{15}N_2O_3$ (MH^+) 211.1083, found 211.1102.

*1-butyl-5-hydroxy-4-oxo-1,4-dihydropyridine-2-carbaldehyde O-ethyl oxime (**9**):*

Yield 61%, white solid. ^{1}H NMR (500 MHz, DMSO-d_6) δ: 0.88 (t, J = 7.5 Hz, 3H, CH_3), 1.29 (t, J = 7.5 Hz, 5H, 2H in CH_2 and 3H in CH_3), 1.62-1.71 (m, 2H, CH_2), 4.28 (q, J = 7.5 Hz, 2H, CH_2), 4.44 (t, J = 7.5 Hz, 2H, CH_2), 7.66 (s, 1H, C3-H in pyridinone ring), 8.36 (s, 1H, C6-H in pyridinone ring), 8.64 (s, 1H, CH). ^{13}C NMR (125 MHz, DMSO-d_6, δppm) δ: 13.87, 14.82, 19.21, 32.94, 56.19, 71.30, 111.59, 132.72, 138.93, 141.96, 146.50, 160.28. ESI-MS: *m/z* 239 (MH^+), HRMS: *m/z* calcd for $C_{12}H_{19}N_2O_3$ (MH^+) 239.1396, found 239.1421.

*1-hexyl-5-hydroxy-4-oxo-1,4-dihydropyridine-2-carbaldehyde O-ethyl oxime (**10**):*

Yield 63%, white solid. ^{1}H NMR (500 MHz, CD_3OD) δ: 0.92 (t, J = 7.5 Hz, 3H, CH_3), 1.36 (t, J = 7.0 Hz, 9H, 6H in $3CH_2$ and 3H in CH_3), 1.80-1.87 (m, 2H, CH_2), 4.35 (q, J = 7.0 Hz, 2H, CH_2), 4.48 (t, J = 7.5 Hz, 2H, CH_2), 7.56 (s, 1H, C3-H in pyridinone ring), 8.22 (s, 1H, C6-H in pyridinone ring), 8.50 (s, 1H, CH). ^{13}C NMR (125 MHz, CD_3OD) δ: 12.82, 13.41, 22.06, 25.38, 30.57, 30.92, 56.66, 71.33, 111.28, 131.95, 139.79, 140.21,

146.26, 159.80. ESI-MS: *m/z* 267 (MH^+), HRMS: *m/z* calcd for $C_{14}H_{23}N_2O_3$ (MH^+) 267.1709, found 267.1746.

*5-hydroxy-1-octyl-4-oxo-1,4-dihydropyridine-2-carbaldehyde O-ethyl oxime (**11**)*: Yield 70%, white solid. ^{1}H NMR (500 MHz, DMSO-d_6) δ: 0.84 (t, *J* = 7.0 Hz, 3H, CH_3), 1.17-1.26 (m, 10H, $5CH_2$), 1.29 (t, *J* = 7.0 Hz, 3H, CH_3), 1.62-1.72 (m, 2H, CH_2), 4.28 (t, *J* = 7.0 Hz, 2H, CH_2), 4.42 (t, *J* = 7.0 Hz, 2H, CH_2), 7.60 (s, 1H, C-3H in pyridinone ring), 8.32 (s, 1H, C-6H in pyridinone ring), 8.64 (s, 1H, CH). ^{13}C NMR (125 MHz, DMSO-d_6, δppm) δ: 14.36, 14.81, 22.47, 25.79, 28.81, 28.87, 30.90, 31.56, 56.28, 71.27, 111.78, 132.50, 139.00, 142.08, 146.57, 160.67. ESI-MS: *m/z* 295 (MH^+), HRMS: *m/z* calcd for $C_{16}H_{27}N_2O_3$ (MH^+) 295.2022, found 295.2073.

2.3. Tyrosinase Inhibition Assay

*2.3.1. Inhibitory effects of compounds **6**-**11** on mushroom tyrosinase*

Both monophenolase and diphenolase activities of mushroom tyrosinase were determined according to previously reported methods with some modifications by measuring the rate of dopachrome formation at 475 nm (Ling, et al., 2009). In this investigation, the total volume of the reaction system was 300 μL, $_L$-Tyr and $_L$-DOPA were used as the substrate for the determination of monophenolase and diphenolase activity, respectively. Briefly, $_L$-Tyr (100 μL, 2 mM) or $_L$-DOPA (100 μL, 0.5 mM), phosphate buffer (180 μL, pH 6.86, 50 mM) and different concentrations of inhibitor (10 μL in DMSO) were mixed and incubated at 30 ^{o}C. Then, an aqueous solution of

mushroom tyrosinase (10 μL, 2000 U/mL) was added to the above solution and mixed quickly. The final concentration of DMSO in the test solution was 3.3%. Absorption and kinetic measurements were carried out on an Infinite M200 Multi-Detection Microplate Reader from TECAN at 475 nm. Control containing the same amount of DMSO without inhibitor, was routinely carried out. All the measurements were performed in triplicate.

2.3.2. Assay of the Inhibition Type and Inhibition Constant

The inhibition type was assayed by the Lineweaver-Burk plot based on the results of inhibitory effect on the diphenolase activity of tyrosinase, and the inhibition constant was determined by the secondary plots of the apparent K_m/V_m or $1/V_m$ versus the concentration of the inhibitor, as described by Chen et al (Chen, Chen, Qiu, Song, & Huang, 2003).

2.4. Molecular docking study

Molecular docking was performed by using CDOCKER module embedded in Discovery Studio 2.5 software (Accelrys Software, Inc., San Diego, CA, USA). The X-ray crystal structure of tyrosinase from *Agaricus bisporus* (PDB ID: 2Y9X) was retrieved from the Protein Data Bank (http://www.rcsb.org/pdb). 3D structures of compounds were built in Chem3D Ultra 8.0, and conformations were generated by using a modified CHARMm force field. The obtained conformations were then docked into the binding site of

tyrosinase. The final binding conformation of each compound was determined based on calculated -CDOCKER energy and -CDOCKER interaction energy.

2.5. Effect on the browning process of fresh-cut apples

2.5.1. Preparation of fresh-cut apples

'Fuji' apples, which were planted in Luochuan of Shanxi province, China, were purchased from Yonghui supermarket in Hangzhou, Zhejiang province, China. The apples were selected from the same batch with similar size and maturity without injuries, diseases or pests. Apples were cut into pieces (8 mm × 5 mm× 3 mm) by using a sharp knife. About 200 g of apple slices were equally divided into two groups: the control group was dipped in sterile ultrapure water for 60 sec at room temperature and the treatment group was dipped in the solution of compound **11** (0.5 mg/mL) under the same conditions. Samples were then air-dried naturally and immediately packaged into individual polypropylene film bags (about 30 g sample in each bag; 3 bags for control group and 3 bags for treatment group), and stored at 4 ^{o}C for up to 10 days. Since the preliminary study indicated the colors of the control group and treatment group were apparently different after 2 h, the browning indexes for these apple samples after 2 h of slicing were performed as the onset of the measurements. The browning indexes were measured at an interval of 2 days in triplicates.

2.5.2. Color measurement

The color of apple samples was measured using a CR-400 Minolta chronometer instrument (Konica Minolta, Osaka, Japan). Three readings of L^*, a^*, and b^* were recorded for each sample. The L^* value represents lightness; the $+a^*$ and $-a^*$ values represent redness and greenness, respectively. The $+b^*$ and $-b^*$ values represent yellowness and blueness, respectively. The color measurement was performed in triplicates by random sampling.

2.5.3. Determination of the browning indexes

The browning indexes were measured in triplicates according to a reported method (Kim, Kim, Chung, & Moon, 2014). Apple samples (2 g) were homogenised in 40 mL of distilled water and 10 mL of 10% trichloroacetic acid, allowed to stand for 2 h at 35 ^{o}C, and then filtered using filter paper. The absorbance of the filtrate was measured at 420 nm on a UV-2100 spectrophotometer.

2.6. Statistical Analyses

All experiments were performed in triplicate. The data were statistically analyzed using analysis of variance test (SPSS Statistics 19 software). Data in the tables and figures were given as mean ± SD and analyzed by one-way ANOVA. Significant differences between the treatments were examined by Duncan's multiple range test. $P < 0.05$ was considered as statistically significant.

3. Results and discussion

*3.1. Synthesis of compounds **6-11***

Compounds **6**-**11** were synthesized starting from kojic acid (**1**) (Fig. 1). Benzylation of 5-hydroxy group in kojic acid was achieved by the reaction of kojic acid and benzyl chloride under basic condition to provide **2** in good yield. Condensation of **2** with amine generated **3**, which was then selectively oxidized by active manganese (IV) oxide in dichloromethane at 50 ^{o}C, yielding products **4** in a reasonable yield. Compounds **4** were then subsequently converted to their oxime ether derivatives **5** by reaction with ethoxyamine hydrochloride. Deprotection of the benzyl group on **5** was achieved by treating with hydrochloric acid solution at 100 ^{o}C, generating 5-hydroxy-4-oxo-1,4-dihydropyridine-2-carbaldehyde *O*-ethyl oxime **6**-**11**. All the final compounds have been fully characterized by ^{1}H NMR, ^{13}C NMR, MS and HRMS.

*3.2. Inhibitory effect of compounds **6**-**11** on monophenolase activity of mushroom tyrosinase*

All the newly synthesized compounds **6**-**11** were screened for the inhibitory activity on monophenolase of mushroom tyrosinase using $_{L}$-Tyr as a substrate. The IC_{50} values of compounds **6**-**11** against monophenolase activity were shown in Table 1. The inhibitory activity of compounds **6**-**11** follows the order: **11 > 10 > 9 > 8 > 7 > 6**. Compounds **8**-**11** were found to exhibit strong inhibition against monophenolase activity of tyrosinase, with IC_{50} values of 7.45, 4.78, 2.04 and 1.60 μM, respectively. The strongest compound **11**

was 7.7 fold more potent than that of kojic acid (IC_{50} = 12.24 μM), which is stronger than the best hydroxypyidinone derivative in our previous study (6.4 fold more active than kojic acid) (Zhao, et al., 2016).

The *c*log *P* value is an important indicator of lipophilicity. As shown in Table 1, from compounds **6** to **11**, the *c*log *P* values increased due to the increase of carbon chain length at position-1 of pyridine ring (The *c*log *P* values in this article were calculated using the following web software: http://www.molinspiration.com/cgi-bin/properties). The tyrosinase inhibitory activity of these compounds increased with the increase of their *c*log *P* values, which is in good agreement with previous reports (Gaeta, et al., 2011; Li, et al., 2013). Thus, the high activity of compounds **10** and **11** could be attributed to their high lipophilicity, which renders them to enter readily the hydrophobic pocket of at the active site of tyrosinase.

In attempts to search for more potential tyrosinase inhibitors, many kojic acid derivatives have been synthesized. For example, Lee (Lee, Park, Kim, Seo, & Kim, 2006) reported the synthesis of a kojic acid derivative with a potent tyrosinase inhibitory activity (IC_{50} = 3.63 μM), while it needs longer synthetic procedure. Saghaie (Saghaie, Pourfarzam, Fassihi, & Sartippour, 2013) reported some novel derivatives of kojic acid with the lowest IC_{50} value at 0.37 mM. Compared with these compounds, **10** and **11** showed a stronger inhibitory effect. A range of benzaldehyde-*O*-alkyloximes also have been reported to have potent tyrosinase inhibitory activity (Ley & Bertram, 2001), the

most active compound was the 3,4-dihydroxybenzaldehyde-*O*-ethyloxime with an IC_{50} value of 0.3 μM.

In order to further evaluate the inhibitory activity of **10** and **11** on the monophenolase activity, the kinetic courses of the oxidation of L-Tyr catalyzed by mushroom tyrosinase in the presence of different concentrations of **10** and **11** were investigated (Fig. 2). A lag time, characteristic of monophenolase activity, was observed simultaneously with the appearance of the first stable product dopachrome (Chen, et al., 2012). The reaction system reached a steady state after the lag time. After the steady state, the formation of product increased linearly with increasing reaction time (Cui, et al., 2015; Li, et al., 2010). The slope of the line denoted the steady-state rate and the lag time. As shown in Fig. 2, the lag time did not change with increasing inhibitor concentration, but the steady-state rate decreased distinctly and dose-dependently. The results indicated that **10** and **11** could inhibit the monophenolase activity of mushroom tyrosinase by decreasing the steady-state rates of the enzyme without prolonging the lag time.

*3.3. Effect of **10** and **11** on diphenolase activity of mushroom tyrosinase*

The inhibitory activity of **10** and **11** on the diphenolase activity of mushroom tyrosinase was investigated using L-DOPA as a substrate. As shown in Fig. 3a, both **10** and **11** exhibited potent inhibitory effect on diphenolase activity in a dose dependent manner. The IC_{50} values of **10** and **11** on the diphenolase activity of tyrosinase were determined as 13.89 and 7.99 μM, respectively (Table 1). It was also found that there was

no lag time for both compounds **10** and **11** in the progress of enzyme-catalyzed oxidation of L-DOPA (Fig. S1). Some previous reports (Chen, et al., 2012; Li, et al., 2010; Cui, et al., 2015) have also demonstrated that the reaction process catalyzed by the diphenolase activity of tyrosinase had no lag time.

To ascertain the inhibition mechanism on mushroom tyrosinase, the oxidation of L-DOPA in the presence of **10** and **11** was investigated. Fig. 3b shows that the plots of the remaining enzyme activity versus the concentrations of enzyme at different concentrations of **11** gave a family of straight lines, which all passed through the origin. This result is similar to those of previous reports (Chen, et al., 2012; Zhao, et al., 2016). Increase of inhibitor concentration resulted in descent of the slope of the line, indicating that the presence of inhibitor resulted in the inhibition of enzyme activity (Li, et al., 2010). Thus, the inhibition of compounds **11** on diphenolase activity of tyrosinase is reversible. Compound **10** was found to behave in the same manner as that of **11** (Fig. S2).

The inhibition type of **10** and **11** on the oxidation of L-DOPA by tyrosinase was investigated by Lineweaver-Burk double-reciprocal plots. As shown in Fig. 3c, the plots of 1/v versus 1/[S] gave a family of straight lines with different slopes which intercept in the second quadrant, indicating that **11** was a competitive-uncompetitive mixed-type inhibitor. Compound **10** was also determined to be a mixed-type inhibitor (Fig. S3). Thus, both compounds **10** and **11** can bind to either free enzyme or enzyme-substrate complexes. The equilibrium constant for inhibitor binding with free enzyme (K_I) was obtained from a plot of slope (K_m/V_m) versus the concentration of the inhibitor, and that

for binding the enzyme-substrate complex (K_{IS}) was obtained from a plot of the vertical intercept ($1/V_m$) versus the concentration of the inhibitor. The K_I and K_{IS} values of **11** were measured as 18.07 and 21.34 μM, respectively, while those values for **10** being 24.84 and 32.54 μM, respectively. The K_{IS} values of both compounds are larger than the K_I values, indicating that the affinity of the inhibitors for free enzyme is greater than that of enzyme-substrate complex. Meanwhile, both affinity constants of **11** are lower than those for **10**, indicating that **11** possesses superior affinities for both the free enzyme and the enzyme-substrate complex to those of **10**. This result is consistent with their inhibitory effects on tyrosinase activity.

3.4 Molecular docking study

In order to understand the right site and interaction forces of inhibitor binding to tyrosinase, the molecular docking of compounds **11** and **10** to tyrosinase was performed by adopting the CDOCKER. The docking estimation was performed by the -CDOCKER energy and -CDOCKER interaction energy. Higher energy values imply more favorable binding affinities between the protein and the ligand. The -CDOCKER energy values of compounds **11** and **10** were calculated to be 43.0580 and 41.3714, respectively; while the -CDOCKER interaction energy values were calculated to be 45.6179 and 44.2514, respectively. Thus, the docking energies were consistent with their IC_{50} values, which may further explain the better tyrosinase inhibitory activity of compound **11**. The binding mode of compound **11** was provided in Fig. 4. The hydroxypyridinone ring of compound

11 was embedded in the active site of tyrosinase, and the 4,5-dihydroxy moiety coordinated with the copper ion. The aliphatic chain at position-1 and the side chain at position-2 stretched out in a T shape, forming hydrophobic interaction with the active site of tyrosinase, indicating a favorable interaction between compound **11** and tyrosinase.

*3.5. Effect of **11** on controlling the browning of apples*

The browning effect and the loss of color are common characteristics of fresh-cut fruit due to the tissue damage provoked by peeling and slicing, which can induce enzymatic and non-enzymatic browning reactions promoting loss of natural color (Chiumarelli & Hubinger, 2012). In this study, the browning degree of apple was represented as the color value of cut surfaces and the absorbance (browning index) of water extract of apple samples. It is well known that the measurement of L^* and a^* values is a suitable method for evaluating the degree of browning in fruits and vegetables (Castaner, Gil, Ruiz, & Artes, 1999). Lower L^* and higher a^* values indicate that a product becomes more brown. The changes in color values of post-cut apples treated with **11** and control group samples during storage at 4 ^{o}C are shown in Fig. 5. The L^* values of the treatment group and control group were 53.25 and 35.53, respectively, at 2 h after slicing. The differences of L^* values between the treatment group and the control group were significant ($P < 0.05$). The L^* values decreased with the increase of the storage time (Fig. 5a), which indicated that the browning reaction occurred. During the former half test period (0-6 days), the L^* values in the fresh-cut apples treated with **11** were

significantly higher than those of control group ($P < 0.05$). On the day 10, the L^* value of **11**-treated apple slices was close to that of control group. As shown in Fig. 5, a^* and b^* values of both groups increased gradually, while a^* and b^* values of the treatment group were lower than those of control group ($P < 0.05$). The increasing of a^* and b^* values indicated yellowing or loss of green color, which is normally considered to be the consequence of chorophyll degradation (Toivonen & Brummell, 2008).

Surface browning, the major limit for the shelf life of fresh-cut fruit and vegetables, is mainly associated with phenol metabolizing enzymes (Xing, et al., 2015; You, et al., 2012). It is believed that the interaction between enzymes, such as POD and PPO, and phenolic substrates, leads to phenol oxidation (Cantos, Tudela, And, & Espín, 2002). Because phenols are distributed in the vacuole, PPO and POD are located in the cell wall, cell membrane and cytoplasm, this distribution prevents contact between the substrate and the enzyme, thus avoiding the occurrence of enzymatic browning in normal tissues (Xing, et al., 2015; Zhu, Zhou, Zhu, & Guo, 2009). However, fresh-cut fruits and vegetables disrupt this distribution, allowing the phenolic compounds to migrate and react with PPO and POD, thus causing tissue browning (Xing, et al., 2015). In addition, the regional distribution of enzymes and phenolic compounds may prevent the browning occurring inside the apples, which also explains that the L^* values of untreated apple samples remain at 36 without marked decrease after 2 h. In the case of **11**-treated group, the browning of apple slices was delayed during the storage due to the fact that **11** bound the copper ions at the active site of PPO, thereby inhibiting the PPO activity. However, a

wound signal of fresh-cut products that migrates into adjacent, uninjured tissue, induces a number of physiological responses (e.g., oxidative browning, generation of secondary metabolites and lipid degradation), which is controlled by a complicated cascade network (Chen, Xing, Wang, Zheng, & Wang, 2015; Saltveit, 2000; Brecht, 1995).

The browning index was also investigated by measuring the absorbance at 420 nm, which is generally considered to be an indirect measure of the contents of soluble pigment compounds produced from browning reactions (Kim, Kim, Chung, & Moon, 2014). The results of browning index of the treatment group and control group are shown in Fig. 5d. The absorbance values of both groups at 420 nm were increased during the storage time. However, the browning index of **11**-treated group was significant lower than that of the control group ($P < 0.05$). The results of browning index test are in good agreement with those of color measurement.

4. Conclusions

A range of hydroxypyridinone derivatives containing an oxime ether moiety were synthesized in this study. Among them, **11** showed the highest inhibitory effect against mushroom tyrosinase. Kinetic investigation demonstrated that **11** is a reversible and mixed type inhibitor against diphenolase activity of mushroom tyrosinase. **11** can effectively prolong the shelf-life of fresh-cut apple slices by retarding browning. Thus, such compounds could find applications in food preservation.

Supplementary materials

The data for the inhibition kinetics of **10** and **11** on diphenolase activity of tyrosinase, determination of inhibition mechanism of **10** on mushroom tyrosinase and its Lineweaver-Burk plots are presented in Supplementary materials.

Acknowledgements

The authors thank Zhejiang Provincial Natural Science Foundation of China (No. LY17B020001) and Postgraduate Science and Technology Innovation Project from Zhejiang Gongshang University.

References

Allende, A., Tomás-Barberán, F. A., & Gil, M. I. (2006). Minimal processing for healthy traditional foods. *Trends in Food Science & Technology, 17*, 513-519.

Brecht, J. K. (1995). Physiology of lightly processed fruits and vegetables. *Hortscience, 30*, 18-22.

Cantos, E., Tudela, J. A., And, M. I. G., & Espín, J. C. (2002). Phenolic compounds and related enzymes are not rate-limiting in browning development of fresh-cut potatoes. *Journal of Agricultural & Food Chemistry, 50*, 3015-3023.

Castaner, M., Gil, M. I., Ruiz, M. V., & Artes, F. (1999). Browning susceptibility of minimally processed Baby and Romaine lettuces. *European Food Research and Technology, 209*, 52-56.

Chang, T. S. (2009). An updated review of tyrosinase inhibitors. *International Journal of Molecular Sciences, 10*, 2440-2475.

Chen, B. J., Zhou, Y. J., Wei, X. Y., Xie, H. J., Hider, R. C., & Zhou, T. (2016). Edible Antimicrobial Coating Incorporating a Polymeric Iron Chelator and Its Application in the Preservation of Surimi Product. *Food & Bioprocess Technology, 9,* 1031-1039.

Chen, B. N., Xing, R., Wang, F., Zheng, A. P., & Wang, L. (2015). Inhibitory effects of α-$Na_8SiW_{11}CoO_{40}$ on tyrosinase and its application in controlling browning of fresh-cut apples. *Food Chemistry, 188*, 177-183.

Chen, L. H., Hu, Y. H., Song, W., Song, K. K., Liu, X., Jia, Y. L., Zhuang, J. X., & Chen, Q. X. (2012). Synthesis and antityrosinase mechanism of benzaldehyde thiosemicarbazones: novel tyrosinase inhibitors. *Journal of Agricultural & Food Chemistry, 60*, 1542-1547.

Chen, Q., Chen, Q. X., Qiu, L., Song, K. K., & Huang, H. (2003). Inhibitory effect of 4-cyanobenzaldehyde and 4-cyanobenzoic acid on mushroom (*Agaricus bisporus*) Tyrosinase. *Journal of Protein Chemistry, 22*, 607-612.

Chiumarelli, M., & Hubinger, M. (2012). Stability, solubility, mechanical and barrier properties of cassava starch – Carnauba wax edible coatings to preserve fresh-cut apples. *Food Hydrocolloids, 28*, 59-67.

Chung, H. S., & Moon, K. D. (2009). Browning characteristics of fresh-cut 'Tsugaru' apples as affected by pre-slicing storage atmospheres. *Food Chemistry, 114*, 1433-1437.

Cui, Y., Liang, G., Hu, Y. H., Shi, Y., Cai, Y. X., Gao, H. J., Chen, Q. X., & Wang, Q. (2015). Alpha-substituted derivatives of cinnamaldehyde as tyrosinase inhibitors: Inhibitory mechanism and molecular analysis. *Journal of Agricultural & Food Chemistry, 63*, 716-722.

Dai, X. Y., Zhang, M. X., Wei, X. Y., Hider, R. C., & Tao Zhou, T. (2016). Novel multifunctional hydroxypyridinone derivatives as potential shrimp preservatives. *Food and Bioprocess Technology*, *9*, 1079-1088.

Gaeta, A., Molina-Holgado, F., Kong, X. L., Salvage, S., Fakih, S., Francis, P. T., Williams, R. J., & Hider, R. C. (2011). Synthesis, physical-chemical characterisation and biological evaluation of novel 2-amido-3-hydroxypyridin-4(1*H*)-ones: Iron chelators with the potential for treating Alzheimer's disease. *Bioorganic & Medicinal Chemistry, 19*, 1285-1297.

Hamidian, H., Tagizadeh, R., Fozooni, S., Abbasalipour, V., Taheri, A., & Namjou, M. (2013). Synthesis of novel azo compounds containing 5(4*H*)-oxazolone ring as potent tyrosinase inhibitors. *Bioorganic & Medicinal Chemistry, 21*, 2088-2092.

İyidoğan, N. F., & Bayındırlı, A. (2004). Effect of $_{L}$-cysteine, kojic acid and 4-hexylresorcinol combination on inhibition of enzymatic browning in Amasya apple juice. *Journal of Food Engineering, 62,* 299-304.

Kim, D. H., Kim, H. B., Chung, H. S., & Moon, K. D. (2014). Browning control of fresh-cut lettuce by phytoncide treatment. *Food Chemistry, 159*, 188-192.

Kim, Y. J., & Uyama, H. (2005). Tyrosinase inhibitors from natural and synthetic sources: structure, inhibition mechanism and perspective for the future. *Cellular & Molecular Life Sciences, 62*, 1707-1723.

Hridya, H., Amrita, A., Mohan, S., Gopalakrishnan, M., Dakshinamurthy, T. K., Doss, G. P., & Siva, R. (2016). Functionality study of santalin as tyrosinase inhibitor: A potential depigmentation agent. *International Journal of Biological Macromolecules, 86*, 383-389.

Kwak, S. Y., Choi, H. R., Park, K. C., & Lee, Y. S. (2011). Kojic acid-amino acid amide metal complexes and their melanogenesis inhibitory activities. *Journal of Peptide Science, 17*, 791–797.

Lee, Y. S., Park, J. H., Kim, M. H., Seo, S. H., & Kim, H. J. (2006). Synthesis of tyrosinase inhibitory kojic acid derivative. *Archiv Der Pharmazie, 339*, 111-114.

Ley, J. P., & Bertram, H. J. (2001). Hydroxy- or methoxy-substituted benzaldoximes and benzaldehyde-*O*-alkyloximes as tyrosinase inhibitors. *Bioorganic & Medicinal Chemistry, 9*, 1879-1885.

Li, D. F., Hu, P. P., Liu, M. S., Kong, X. L., Zhang, J. C., Hider, R. C., & Zhou, T. (2013). Design and synthesis of hydroxypyridinone-$_L$-phenylalanine conjugates as potential tyrosinase inhibitors. *Journal of Agricultural & Food Chemistry, 61*, 6597-6603.

Li, Z. C., Chen, L. H., Yu, X. J., Hu, Y. H., Song, K. K., Zhou, X. W., & Chen, Q. X. (2010). Inhibition kinetics of chlorobenzaldehyde thiosemicarbazones on mushroom tyrosinase. *Journal of Agricultural & Food Chemistry, 58*, 12537-12540.

Ling, Q., Chen, Q. H., Zhuang, J. X., Xue, Z., Zhou, J. J., Guo, Y. J., & Chen, Q. X. (2009). Inhibitory effects of α-cyano-4-hydroxycinnamic acid on the activity of mushroom tyrosinase. *Food Chemistry, 112*, 609–613.

Liu, P., Shu, C., Liu, L., Huang, Q., & Peng, Y. (2016). Design and synthesis of thiourea derivatives with sulfur-containing heterocyclic scaffolds as potential tyrosinase inhibitors. *Bioorganic & Medicinal Chemistry, 24*, 1866-1871.

Mayer, A. M. (2006). Polyphenol oxidases in plants and fungi: going places? A review. *Phytochemistry, 67,* 2318-2331.

Mosneaguta, R., Alvarez, V., & Barringer, S. A. (2012). The effect of antibrowning agents on inhibition of potato browning, volatile organic compound profile, and microbial inhibition. *Journal of Food Science, 77*, C1234–C1240.

Noh, J. M., Kwak, S. Y., Seo, H. S., Seo, J. H., Kim, B. G., & Lee, Y. S. (2009). Kojic acid-amino acid conjugates as tyrosinase inhibitors. *Bioorganic & Medicinal Chemistry Letters, 19*, 5586-5589.

Saghaie, L., Pourfarzam, M., Fassihi, A., & Sartippour, B. (2013). Synthesis and tyrosinase inhibitory properties of some novel derivatives of kojic acid. *Research in Pharmaceutical Sciences, 8*, 233-242.

Saltveit, M. E. (2000). Wound induced changes in phenolic metabolism and tissue browning are altered by heat shock. *Postharvest Biology & Technology, 21*, 61-69.

Shah, H. M. S., Khan, A. S., & Ali, S. (2017). Pre-storage kojic acid application delays pericarp browning and maintains antioxidant activities of litchi fruit. *Postharvest Biology & Technology, 132,* 154-161.

Toivonen, P. M. A., & Brummell, D. A. (2008). Biochemical bases of appearance and texture changes in fresh-cut fruit and vegetables. *Postharvest Biology & Technology, 48*, 1-14.

Tomás-Barberán, F. A., & Espín, J. C. (2001). Phenolic compounds and related enzymes as determinants of quality in fruits and vegetables. *Journal of the Science of Food & Agriculture, 81*, 853–876.

Xing, R., Zheng, A., Wang, F., Wang, L., Yu, Y., & Jiang, A. (2015). Functionality study of $Na_6PMo_{11}FeO_{40}$ as a mushroom tyrosinase inhibitor. *Food Chemistry, 175*, 292-299.

Xu, L. L., Hu, P. P., Kong, X. L., Hider, R. C., Zhou, T., & Dai, Z. Y. (2014). 3-Hydroxypyridinone-$_L$-phenylalanine conjugates with antimicrobial and tyrosinase inhibitory activities as potential shrimp preservatives. *International Journal of Food Science & Technology, 49,* 797–803.

You, Y., Jiang, Y., Sun, J., Liu, H., Song, L., & Duan, X. (2012). Effects of short-term anoxia treatment on browning of fresh-cut Chinese water chestnut in relation to antioxidant activity. *Food Chemistry, 132*, 1191-1196.

Zhao, D. Y., Zhang, M. X., Dong, X. W., Hu, Y. Z., Dai, X. Y., Wei, X., Hider, R. C., Zhang, J. C., & Zhou, T. (2016). Design and synthesis of novel hydroxypyridinone derivatives as potential tyrosinase inhibitors. *Bioorganic & Medicinal Chemistry Letters, 26*, 3103-3108.

Zheng, Z. P., Zhang, Y. N., Zhang, S., & Chen, J. (2016). One-pot green synthesis of 1,3,5-triarylpentane-1,5-dione and triarylmethane derivatives as a new class of tyrosinase inhibitors. *Bioorganic & Medicinal Chemistry Letters, 26*, 795-798.

Zhu, L. Q., Zhou, J., Zhu, S. H., & Guo, L. H. (2009). Inhibition of browning on the surface of peach slices by short-term exposure to nitric oxide and ascorbic acid. *Food Chemistry, 114*, 174-179.

Figure captions

Fig. 1. Chemical reactions for the synthesis of hydroxypyridinone derivatives **6**-**11** from kojic acid (**1**). (a) BnCl, MeOH/H_2O, 70 ^oC, 6 h, 80% yield; (b) $NH_3 \cdot H_2O$, EtOH, reflux, overnight, 76% yield; RNH_2 (R =CH_3, C_2H_5, n-C_4H_9, n-C_6H_{13}, n-C_8H_{17}), EtOH/H_2O, NaOH, reflux, 3 h, 62-74% yield; (c) MnO_2, CH_2Cl_2, 50 ^oC, 3 days, 61-78% yield; (d) $H_2NOC_2H_5 \cdot HCl$, EtOH/H_2O, NaOH, room temperature, 2 h, 61-74%; (e) HCl, MeOH, reflux, 36-72 h, 61-86% yield.

Fig. 2. Inhibitory effects of **10** (A) and **11** (B) on monophenolase activity of mushroom tyrosinase. (a) progress curves for the oxidation of L-Tyr by the enzyme; (b) effects on the steady state rate (curve □) and on the lag time (curve □) for the oxidation of tyrosinase. The concentration of **10** and **11** for curves 1-6 were 0, 1.04, 2.08, 4.17, 8.33 and 16.67 μM, respectively.

Fig. 3. Inhibition on diphenolase activity of mushroom tyrosinase. (a) Inhibitory effect of **10** and **11** on diphenolase activity. (b) Inhibitory mechanism of **11** on diphenolase activity. The concentrations of **11** for curves 1-6 were 0, 4.17, 8.33, 16.67, 25.00 and 33.33 μM, respectively. (c) Lineweaver-Burk plots for inhibition of **11** on mushroom tyrosinase. The concentrations of **11** for curves 1-5 were 0, 8.33, 16.67, 25.00 and 33.33 μM, respectively. (d) The plot of slope versus the concentration of **11** for determining the inhibition

constants K_I. (e) The plot of intercept versus the concentration of inhibitors for determining the inhibition constants K_{IS}.

Fig. 4. Configuration for the interaction of compound **11** with tyrosinase.

Fig. 5. Effect of **11** in controlling the browning of fresh-cut apple slices during the 10 day-storage at 4 ^{o}C. (a) L^*; (b) a^*; (c) b^*; (d) browning index. Means ± SD (n = 3) with different letters in the same chart are significantly different ($P < 0.05$).

Fig. 1.

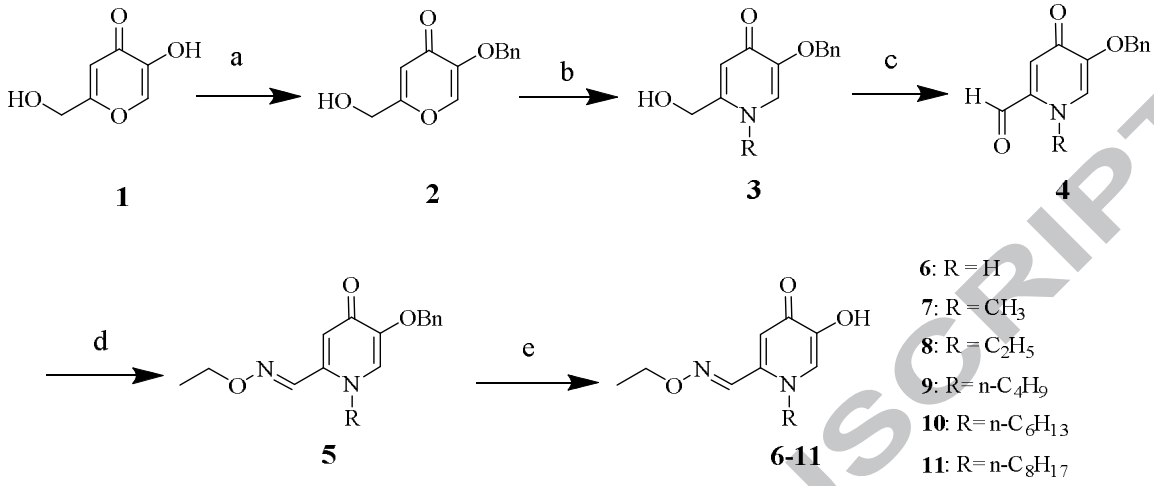

Fig. 2.

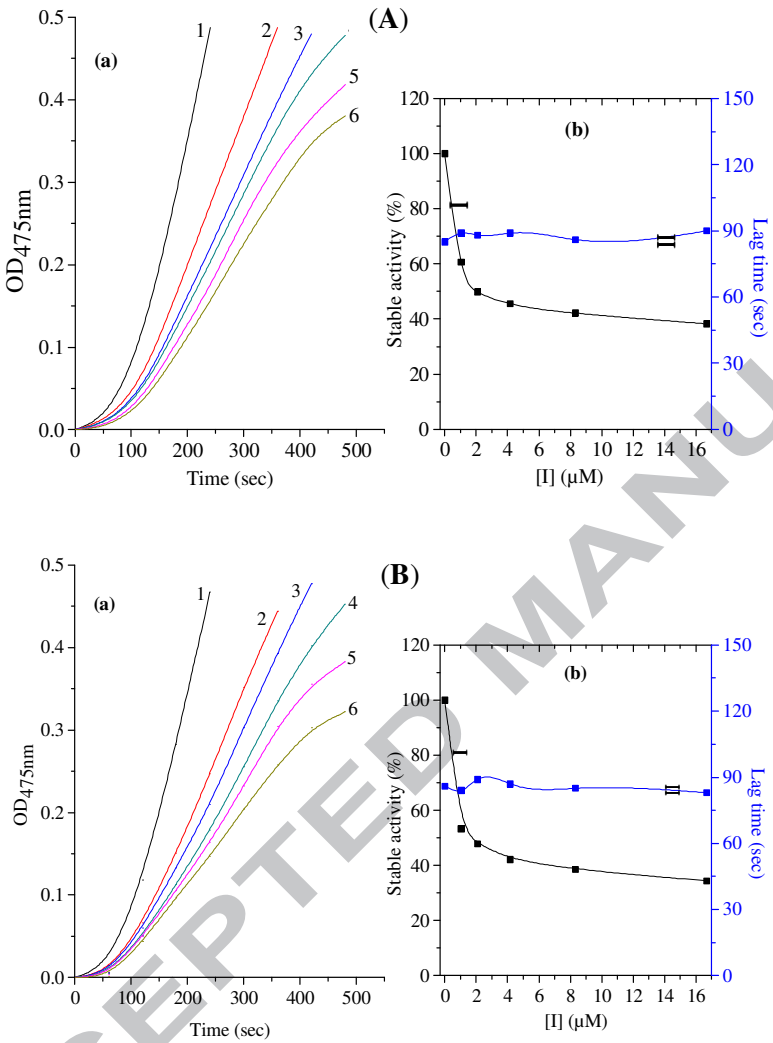

Fig. 3.

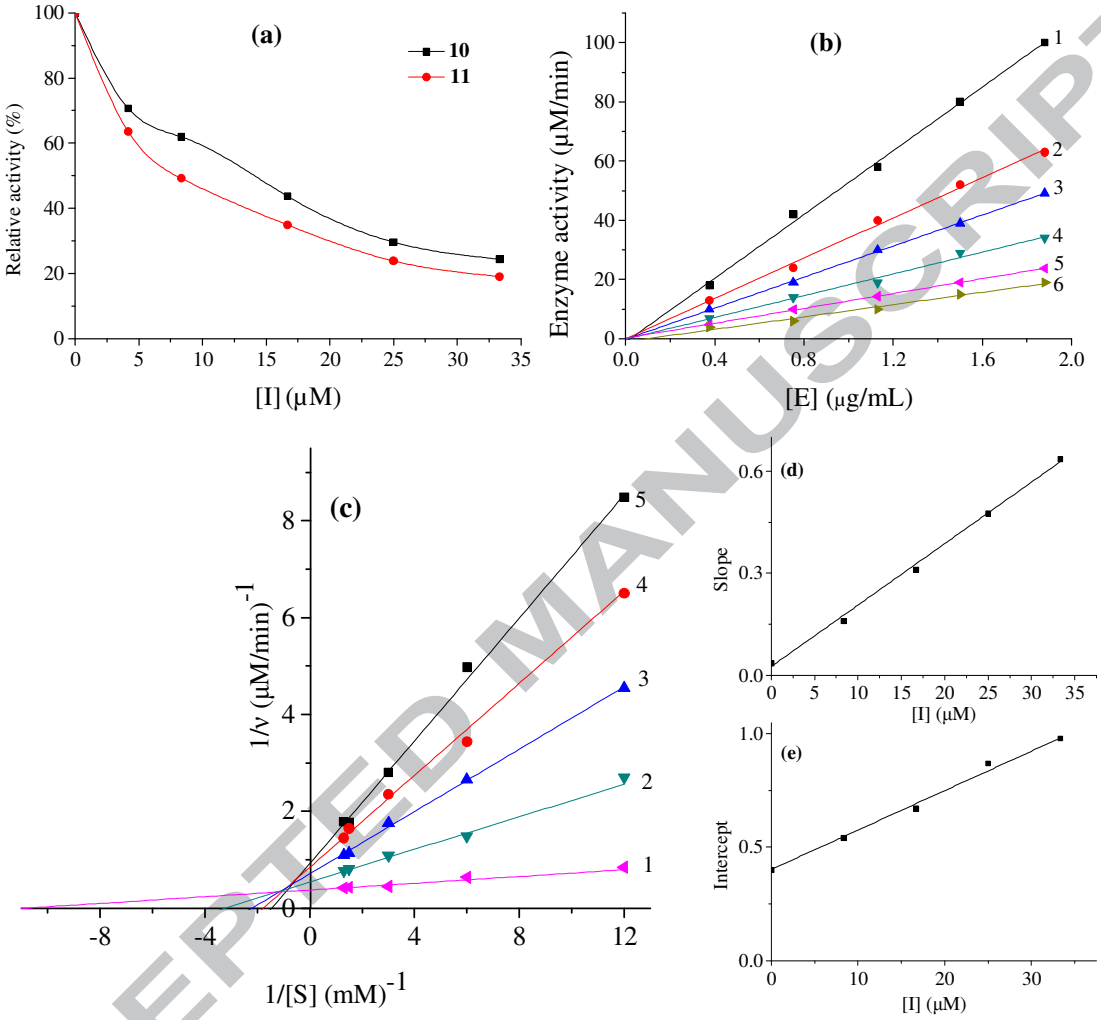

Fig. 4.

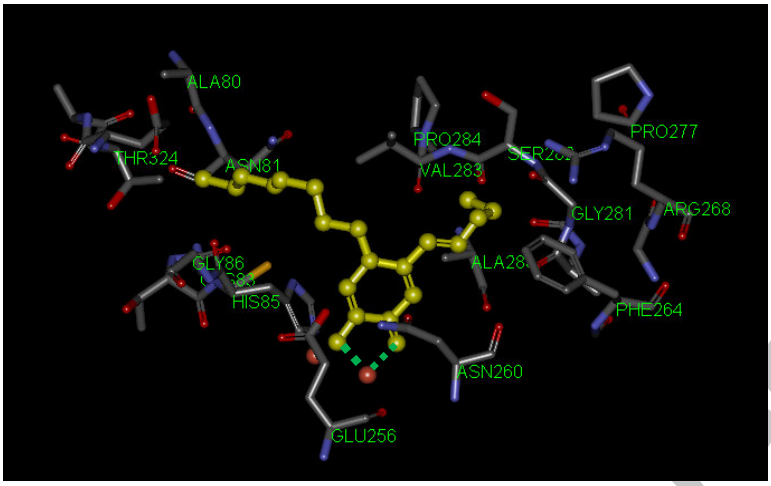

Fig. 5.

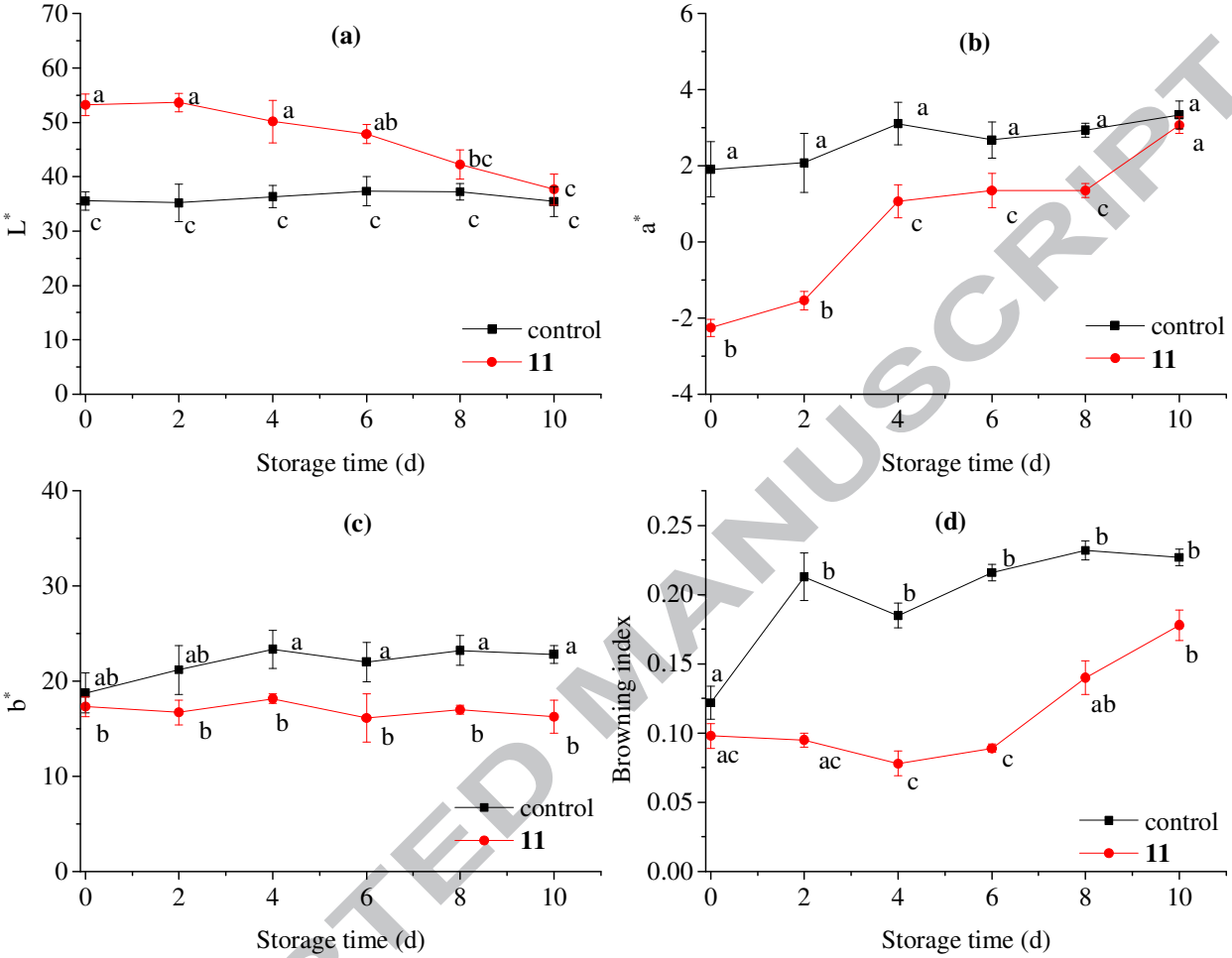

Tables

Table 1. Inhibitory effects of compounds **6-11** on monophenolase and diphenolase activities of mushroom tyrosinase.

Compounds	*C*log *P*	IC_{50} (μM) (monophenolase)	IC_{50} (μM) (diphenolase)
6	-0.16	22.87 ± 1.91	
7	-0.09	19.65 ± 2.03	
8	0.28	7.45 ± 0.87	
9	1.35	4.78 ± 0.43	
10	2.36	2.04 ± 0.12	13.89 ± 1.26
11	3.37	1.60 ± 0.13	7.99 ± 0.67
kojic acid	-0.89	12.24 ± 1.74	

Highlights

- A range of novel hydroxypyridinones containing an oxime ether moiety were synthesized.
- Some molecules exhibited a potent inhibitory activity on mushroom tyrosinase.
- **11** was demonstrated to effectively control the browning of fresh-cut apple slices.